American Mineralogist, Volume 97, pages 1591–1597, 2012

Synthetic B-rich olenite: Correlations of single-crystal structural data† 🔓

Andreas Ertl,[1,*] Gerald Giester,[1] Thomas Ludwig,[2] Hans-Peter Meyer,[2] and George R. Rossman[3]

[1]Institut für Mineralogie und Kristallographie, Geozentrum, Universität Wien, Althanstrasse 14, 1090 Vienna, Austria
[2]Institut für Geowissenschaften, Universität Heidelberg, Im Neuenheimer Feld 236, 69120 Heidelberg, Germany
[3]Division of Geological and Planetary Sciences, California Institute of Technology, Pasadena, California 91125-2500, U.S.A.

Abstract

Synthetic Al- and B-rich tourmaline crystals described by London (2011) were characterized further by SIMS and new EMP analyses. These tourmalines are the first synthetic B-rich olenites characterized by single-crystal X-ray diffraction, because they are significantly larger than synthetic samples produced in the past. The average final formulas are $^{X}(Na_{0.7}\square_{0.3})^{Y}(Al_{2.5}Li_{0.4}Fe^{2+}_{0.1})^{Z}Al_6(BO_3)_3[Si_{5.2}B_{0.5}Al_{0.3}O_{18}]^{V}[(OH)_{2.9}O_{0.1}]^{W}[O_{0.9}(OH)_{0.1}]$, with $a = 15.765(1)$, $c = 7.083(1)$ Å, $^{X}(Na_{0.7}\square_{0.3})^{Y}(Al_{2.5}Li_{0.5})^{Z}Al_6(BO_3)_3[Si_{4.8}B_{0.9}Al_{0.3}O_{18}]^{V}(OH)_3{}^{W}[(OH)_{0.5}O_{0.5}]$, with $a = 15.746(1)$, $c = 7.075(1)$ Å, and $^{X}(Na_{0.6}Ca_{0.1}\square_{0.3})^{Y}(Al_{2.3}Li_{0.5}Fe_{0.2})^{Z}Al_6(BO_3)_3[Si_{4.7}B_{1.2}Al_{0.2}O_{18}]^{V}(OH)_3{}^{W}[(OH)_{0.9}O_{0.1}]$, with $a = 15.723(1)$, $c = 7.068(1)$ Å. The small <T-O> distances, down to 1.599 Å, reflect relatively high amounts of $^{[4]}$B (up to ~1.2 apfu; refinements with R = ~2%). All these samples also contain significant amounts of $^{[4]}$Al (~0.2 apfu). A pronounced negative correlation ($r^2 = 1.00$; only three data points) between temperature during crystal growth (at a constant pressure) and $^{[4]}$B (from refinement) in these synthetic olenites was found.

Keywords: Synthetic tourmaline, olenite, tetrahedral boron, single-crystal X-ray diffraction

Introduction

In tourmaline, $XY_3Z_6(BO_3)_3T_6O_{18}V_3W$ (X site: usually Na, Ca, vacancy; Y site: usually Al, Li, Mg, Mn, Fe; Z site: usually Al, Mg, Fe; Hawthorne and Henry 1999), the T site usually is occupied by Si and sometimes also by small amounts of Al and B (e.g., Foit, and Rosenberg 1979; Foit 1989; Hawthorne et al. 1993; MacDonald and Hawthorne 1995; Ertl et al. 1997, 2003, 2005, 2006, 2007, 2008; Hughes et al. 2000; Schreyer et al. 2000, 2002; Lussier et al. 2008, 2009). $^{[4]}$Boron increases with the Al content at the Y site approximately as a power function with a linear term up until $^{[4]}B \approx Si \approx 3$ apfu and $^{Y}Al \approx 3$ apfu, respectively, in natural and synthetic Al-rich tourmalines (Ertl et al. 2008). The occurrence of $^{[4]}$B is only possible in solid solutions between the end-members schorl, "oxy-schorl," elbaite, liddicoatite, or rossmanite and hypothetical $^{[4]}$B-rich tourmaline end-members with only Al^{3+} at the Y site (Ertl et al. 2008). By plotting the $^{[4]}$B content of synthetic and natural Al-rich tourmalines, which crystallized at elevated *PT* conditions, it is obvious that there are pronounced correlations between *PT* conditions and the $^{[4]}$B content. Toward lower temperatures higher $^{[4]}$B contents are found in tourmaline, which is consistent with previous investigations on the coordination of B in melts (Ertl et al. 2008). Above a pressure of ~1000–1500 MPa (depending on the temperature), the highest observed $^{[4]}$B content does not change significantly at a given temperature (Ertl et al. 2008). It is still not easy to verify the presence of B at the T site. Especially just by using only electron microprobe data (without measuring B), as it is usually done, tetrahedrally coordinated B can be overlooked. The incorporation of B at the T site in tourmaline can be important for the petrology because it indicates lower temperatures and higher pressures during crystallization (Schreyer et al. 2000; Ertl et al. 2008). The first time synthetic Al-rich tourmaline with verified $^{[4]}$B was described, was by Schreyer et al. (2000). They successfully synthesized tourmaline between 550 °C/1000 MPa and 900 °C/5000 MPa. The crystals were ≤1 μm in the length. At lower pressures of ≤500 MPa they did not successfully produce tourmaline. Similar tourmalines were also synthesized by Schlager (2003) and Kempl (2008). In this work, we examine the chemistry and atomic site-occupancies (by single-crystal X-ray diffraction) of synthetic tourmaline with significant amounts of B at the T site.

Experimental details

Tourmaline synthesis

Three synthetic crystals were provided for this study by David London (University of Oklahoma). These represent preliminary steps in an experimental program (series ElbK) by D. London, Brandon M. Guttery, and George B. Morgan VI (all at University of Oklahoma) to synthesize Li-rich tourmaline as the basis for elucidating the stability field of elbaite. Preliminary observations, along with electron microprobe analyses (EPMA) of ElbK-9 and similar samples, were published in Table 2 of London (2011) and discussed further by London and Morgan (2011). Although London (2011) includes B in the EPMA, the Li and H contents were calculated and undetermined, respectively. London (2011) and London and Morgan (2011) noted that the (calculated) Li content increases with increasing *P* and *T*, while the apparent B content in the tetrahedral site increases with decreasing *T*.

Sample ElbK-13 was synthesized at 600 °C, ElbK-9 at 500 °C, and ElbK-11 at 400 °C (all at 260 MPa H_2O). London used fragments of idiomorphic schorl crystals (dark reddish-brown in transmitted plane-polarized light along the **a**-axis

* E-mail: andreas.ertl@a1.net

† 🔓 Open Access, thanks to the authors' funding. Article available to all readers via GSW (http://ammin.geoscienceworld.org) and the MSA web site.

direction, ~ 0.5 × 2 × 3 mm) from miarolitic cavities at the Hercules pegmatite mine (Ramona District, San Diego Co., California) as seed crystals (D. London, personal communication, 2011). Some additional details of the experimental synthesis are presented in London (2011).

Chemical analyses

The tourmaline crystal fragments used for the structure refinement were prepared as a section (polished on one side of the sample) for chemical analyses. Concentrations of all elements except B, Li, and H were determined with a Cameca SX51 electron microprobe (EPMA) equipped with five wavelength-dispersive spectrometers (University of Heidelberg). The operating conditions were 15 kV accelerating voltage, 20 nA beam current, with a beam diameter of 5 µm. Peaks for all elements were measured for 20 s, except for Zn*K*α (30 s) and F*K*α (40 s). Because the F*K*α line interferes with the Fe and Mn *L*α lines, the measured F values require a correction (Ertl et al. 2009). We used the following (natural and synthetic) standards and X-ray lines for calibration: albite (Na*K*α), periclase (Mg*K*α), corundum (Al*K*α), wollastonite (Si*K*α), rutile (Ti*K*α), scapolite (Cl*K*α), orthoclase (K*K*α), wollastonite (Ca*K*α), hematite (Fe*K*α), rhodonite (Mn*K*α), gahnite (Zn*K*α), and topaz (F*K*α). The analytical data were reduced and corrected using the PAP routine (Pouchou and Pichoir 1985). A modified matrix-correction was applied assuming a stoichiometric proportion of O atoms and all non-measured components were assumed to be B_2O_3. Under the described conditions, analytical errors on all analytical results are ±1% relative for major elements and ±5% relative for minor elements.

Concentrations of H, Li, and B were determined by secondary ion mass spectrometry (SIMS) with a CAMECA ims 3f ion microprobe (University of Heidelberg). Primary O^{2-} ions were accelerated to 14.5 keV, whereas secondary ions were accelerated to a nominal of 4.5 keV. An offset of 75 V was applied to the secondary accelerating voltage so that secondary ions with an initial energy of 75 ± 20 eV were analyzed (energy-filtering). The offset is chosen to minimize possible matrix effects for Li, B (Ottolini et al. 1993), and H.

For Li and B the primary beam current was 10 nA, resulting in a beam diameter of ~ 20 µm. The spectrometer's mass resolution M/ΔM was set to ~1100 (±10%) to suppress interferences and the imaged field was 150 µm in diameter.

For determination of H, the primary beam current was 20 nA, M/ΔM was set to ~400 (±10%) and the imaged field was set to 25 µm (nominal value). To reduce the influence of in situ contamination with water, a small field-aperture (d = 400 µm) was chosen, which limited the analyzed area to ~ 5 µm in diameter. The partial pressure of H_2O in the sample chamber was reduced using the LN_2 cold trap and magnetic field coils were used to compensate magnetic fields near the sample. Due to the high-H concentration in tourmaline, it was not necessary to analyze with multiple values for the primary beam current as described in Ludwig and Stalder (2007), in which the method applied for this work is documented.

The relative ion yield (RIY) for B and H was determined using three tourmaline crystals as reference material (Dyar et al. 1998, 2001). For Li, the standard glass SRM610 (NIST) was used as reference material; concentrations (preferred averages) for Li and Be were taken from Pearce et al. (1997). The RIYs of Li and B were corrected for the Fe + Mn concentration in the samples and in the reference materials, respectively (Ottolini and Hawthorne 1999). Although the matrix of SRM610 is very different from that of tourmalines, it has two distinct advantages for Li-determination: it is homogeneous and its Li concentration is very well determined (see also Ertl et al. 2009). Using the three tourmalines as reference material, a correlation of RIY(H) with the concentration of monovalent cations (Li, Na, K) in the tourmaline was observed. The RIYs were corrected for that correlation.

The relative precision (1σ) of single H, Li, and B SIMS analyses on all samples and reference materials was better than 1%. Matrix effects and the uncertainty of the elemental concentrations in the reference materials limit the accuracy and thus dominate the uncertainty of the SIMS analyses. Based on Ottolini et al. (1993), Ottolini and Hawthorne (1999), and our own observations, the worst-case deviation in the accuracy is estimated with ≤30% for H, ≤20% for Li, and ≤10% for B. Table 1 contains complete chemical-analytical data for the tourmalines.

Crystal structure of B-rich tourmaline

The tourmaline fragments were studied on a Kappa APEX II CCD diffractometer from Bruker AXS equipped with a monocapillary optics collimator and graphite-monochromatized Mo*K*α radiation. Single-crystal X-ray diffraction data (up to 80 °2θ) were collected at room temperature, integrated, and corrected for Lorentz and polarization factors and absorption correction by evaluation of partial multiscans. The structure was refined with SHELXL-97 (Sheldrick 1997) using scattering factors for neutral atoms and a tourmaline-starting model from Ertl et al. (2008). The H atom bonded to the O3 atom was located from a difference-Fourier map and subsequently refined. Refinement was performed with anisotropic displacement parameters for all non-hydrogen atoms. Table 2 provides crystal data and details of the structure refinement. Site occupancies were refined according to well-known characteristics of the tourmaline structure (Na was refined at the X site, Al and Li were refined at the Y site, Si and B were refined at the T site; for other details see Table 3). The refinements converged at *R*1(*F*) values of ~2% (Table 2). In Table 3, we list the atomic parameters and equivalent isotropic displacement parameters, and in Table 4 we present selected interatomic distances.

TABLE 1. Composition of synthetic B-rich olenite (wt%)

	ElbK-13*	ElbK-13†	ElbK-9*	ElbK-9†	ElbK-11‡	ElbK-11†
SiO_2	33.15(18)	33.15	30.95(39)	30.95	29.84(35)	29.86
TiO_2	0.22(2)	0.22	0.28(3)	0.28	0.13(2)	0.13
B_2O_3	13.85(19)	13.07	15.20(15)	14.52	15.66	15.58
Al_2O_3	47.84(25)	47.25	48.30(30)	47.47	46.38(38)	45.69
FeO	0.49(3)	0.49	0.19(3)	0.19	1.66(15)	1.66
MgO	0.02(1)	0.02	b.d.	b.d.	0.07(2)	0.07
ZnO	0.04(1)	0.04	0.04(1)	0.04	0.18(3)	0.18
CaO	0.04(1)	0.04	0.04(1)	0.04	0.24(4)	0.24
Na_2O	2.14(4)	2.14	2.29(10)	2.29	2.09(9)	2.09
Li_2O	0.70(2)	0.70	0.84(3)	0.84	0.78	0.78
F	b.d.	b.d.	0.02(1)	0.02	0.04(2)	0.04
H_2O	2.31(8)	2.88	2.26(9)	3.37	2.67	3.70
O≡F	–	–	–0.01	–0.01	–0.02	–0.02
Sum	100.80	100.00	100.42	100.00	99.72	100.00
N	31	31	31	31	31	31
Si	5.17	5.20	4.83	4.82	4.70	4.65
$^{[4]}$B	0.73	0.54	1.09	0.90	1.26	1.19
$^{[4]}$Al	0.10	0.26	0.08	0.28	0.04	0.16
Sum T site	6.00	6.00	6.00	6.00	6.00	6.00
$^{[3]}$B	3.00	3.00	3.00	3.00	3.00	3.00
^{Z}Al	6.00	6.00	6.00	6.00	6.00	6.00
^{Y}Al	2.69	2.47	2.80	2.42	2.57	2.23
Fe^{2+}	0.06	0.06	0.02	0.02	0.22	0.22
Mg	–	–	–	–	0.02	0.02
Zn	–	–	–	–	0.02	0.02
Li	0.44	0.44	0.53	0.53	0.49	0.49
Ti^{4+}	0.03	0.03	0.03	0.03	0.02	0.02
Sum Y site	3.22	3.00	3.38	3.00	3.34	3.00
Na	0.65	0.65	0.69	0.69	0.64	0.63
Ca	0.01	0.01	0.01	0.01	0.04	0.04
□	0.34	0.34	0.30	0.30	0.32	0.33
Sum X site	0.66	0.66	0.70	0.70	0.68	0.67
Sum cations	18.88	18.66	19.08	18.70	19.02	18.67
OH	2.40	3.00	2.35	3.50	2.80	3.85
F	–	–	0.01	0.01	0.02	0.01
Sum OH + F	2.40	3.00	2.36	3.51	2.82	3.86

* Average of 30 EMP analyses and 2 SIMS analyses for B_2O_3, Li_2O, and H_2O (standard deviation in parentheses).
‡ Average of 10 EMP analyses and 1 SIMS analysis for B_2O_3, Li_2O, and H_2O.
† Weight percent calculated from optimal site occupancies (see text) and normalized to 100%. Cl, MnO, and K_2O are below detection (b.d.) limit. Total Fe was calculated as FeO. A component is not considered significant unless its value exceeds the uncertainty.

IR spectroscopy

We also tried an experimental method, which is still under development using the integrated intensity of the OH bands in the 7000 cm^{-1} region of the infrared spectrum. An approximately 0.4 × 0.8 mm crystal fragment of the most B-rich tourmaline sample investigated (ElbK-11; GRR 3048) was prepared as a doubly polished 0.272 mm thick thin-section. Spectra are obtained on an oriented single crystal in the **E****c** and **E**⊥**c** directions (on a 150 × 60 µm area). The total integrated area (**E****c** + 2×**E**⊥**c**) was then determined (Fig. 1). Because the experimental sample contains numerous cracks and imperfections, the near-IR spectra cannot be used for rigorous quantitative interpretation, but do provide qualitative insight into the amount and type of OH groups.

TABLE 2. Crystal data and results of structure refinement for synthetic B-rich olenite

Sample	ElbK-13	ElbK-9	ElbK-11
a (Å)	15.765(1)	15.746(1)	15.723(1)
c (Å)	7.083(1)	7.075(1)	7.068(1)
V (Å^3)	1524.5(3)	1519.1(3)	1513.2(3)
Crystal dimensions (mm)	0.12 × 0.12 × 0.13	0.07 × 0.10 × 0.15	0.05 × 0.05 × 0.07
Reflections used for determination of unit-cell parameters	11723	7202	3769
$2\theta_{max}$ (°)	79.97	79.43	82.89
h, *k*, *l* ranges	−28/28, −28/28, −12/12	−19/19, −22/22, −9/9	−21/20, −20/21, −9/9
Number of frames	708	506	525
Total reflections measured	24402	13023	13090
Unique reflections	2259	1086	1081
*R*1*(*F*), *wR*2† (*F*^{2}), R_{int}‡ (%)	1.81, 4.05, 2.63	2.07, 5.77, 4.02	2.21, 5.14, 3.45
Flack *x* parameter	0.005(67)	−0.11(17)	−0.22(18)
Observed refls. [$F_o > 4\sigma(F_o)$]	2165	1076	1059
Extinct. coefficient	0.00000(13)	0.00000(25)	0.00000(17)
No. of refined parameters	95	95	95
Goodness-of-fit§	1.056	1.181	1.181
$\Delta\sigma_{min}$, $\Delta\sigma_{max}$ (e/Å^3)	−0.29, 0.46	−0.30, 0.41	−0.34, 0.40

Note: X-ray radiation: Mo*K*α (λ = 0.71073 Å); *Z* = 3; space group: *R*3*m* (no. 160); multi-scan absorption correction (Otwinowski et al. 2003); refinement on *F*^{2}. Frame width, scan time, detector distance: 2°, 60 s (ElbK-11: 100 s), 35 mm. Scan mode: sets of ω and θ scans.
* $R1 = \Sigma||F_o| - |F_c||/\Sigma|F_o|$.
† $wR2 = \{\Sigma[w(F_o^2 - F_c^2)^2]/\Sigma[w(F_o^2)^2]\}^{1/2}$.
$w = 1/[\sigma^2(F_o^2) + (aP)^2 + bP]$, $P = [2F_c^2 + \mathrm{Max}(F_o^2,0)]/3$.
‡ $R_{int} = \Sigma|F_o^2 - F_o^2(\mathrm{mean})|/\Sigma[F_o^2]$.
§ $\mathrm{GooF} = S = \{\Sigma[w(F_o^2 - F_c^2)^2]/(n-p)\}^{1/2}$.

TABLE 3. Positional parameters and their estimated standard deviations for synthetic B-rich olenite

Site	Sample	x	y	z	U_{eq}	Occ.
X	ElbK-13	0	0	0.2392(3)	0.0277(6)	$Na_{0.68(1)}$
	ElbK-9	0	0	0.2397(6)	0.041(1)	$Na_{0.79(1)}$
	ElbK-11	0	0	0.2432(7)	0.039(2)	$Na_{0.76(1)}$
Y	ElbK-13	0.12133(3)	1/2x	−0.34124(6)	0.0072(1)	$Al_{0.87(1)}Li_{0.13}$
	ElbK-9	0.12148(8)	1/2x	−0.3407(2)	0.0106(4)	$Al_{0.85(1)}Li_{0.15}$
	ElbK-11	0.12201(8)	1/2x	−0.3411(2)	0.0102(3)	$Al_{0.88(1)}Li_{0.12}$
Z	ElbK-13	0.29657(2)	0.25998(2)	−0.37354(4)	0.00643(5)	$Al_{1.00}$
	ElbK-9	0.29689(5)	0.26026(5)	−0.3731(1)	0.0070(2)	$Al_{1.00}$
	ElbK-11	0.29718(5)	0.26055(5)	−0.3728(1)	0.0065(2)	$Al_{1.00}$
B	ElbK-13	0.10908(5)	2x	0.4714(2)	0.0062(2)	$B_{1.00}$
	ElbK-9	0.1088(1)	2x	0.4725(4)	0.0070(6)	$B_{1.00}$
	ElbK-11	0.1088(1)	2x	0.4730(5)	0.0078(6)	$B_{1.00}$
T	ElbK-13	0.19135(2)	0.18954(2)	0.02084(3)	0.00413(7)	$Si_{0.909(4)}B_{0.091}$
	ElbK-9	0.19101(4)	0.18941(5)	0.02007(9)	0.0063(2)	$Si_{0.849(4)}B_{0.151}$
	ElbK-11	0.19084(5)	0.18941(5)	0.01968(9)	0.0060(2)	$Si_{0.800(4)}B_{0.200}$
H3	ElbK-13	0.252(2)	1/2x	0.406(4)	0.046(9)	$H_{1.00}$
	ElbK-9	0.248(4)	1/2x	0.420(7)	0.03(1)	$H_{1.00}$
	ElbK-11	0.252(4)	1/2x	0.430(7)	0.03(2)	$H_{1.00}$
O1	ElbK-13	0	0	−0.2107(2)	0.0134(3)	$O_{1.00}$
	ElbK-9	0	0	−0.2076(6)	0.0154(8)	$O_{1.00}$
	ElbK-11	0	0	−0.2049(6)	0.0185(9)	$O_{1.00}$
O2	ElbK-13	0.06016(3)	2x	0.5114(1)	0.0099(2)	$O_{1.00}$
	ElbK-9	0.06004(8)	2x	0.5126(3)	0.0108(5)	$O_{1.00}$
	ElbK-11	0.06004(8)	2x	0.5116(3)	0.0121(5)	$O_{1.00}$
O3	ElbK-13	0.12923(7)	1/2x	−0.4728(1)	0.0107(2)	$O_{1.00}$
	ElbK-9	0.2594(2)	1/2x	−0.4723(3)	0.0114(5)	$O_{1.00}$
	ElbK-11	0.2606(2)	1/2x	−0.4717(3)	0.0122(5)	$O_{1.00}$
O4	ElbK-13	0.09466(4)	2x	0.0950(1)	0.0115(2)	$O_{1.00}$
	ElbK-9	0.09423(9)	2x	0.0933(3)	0.0136(5)	$O_{1.00}$
	ElbK-11	0.0939(1)	2x	0.0917(3)	0.0144(5)	$O_{1.00}$
O5	ElbK-13	0.18657(8)	1/2x	0.1166(1)	0.0123(2)	$O_{1.00}$
	ElbK-9	0.1860(2)	1/2x	0.1158(3)	0.0149(5)	$O_{1.00}$
	ElbK-11	0.1858(2)	1/2x	0.1146(3)	0.0165(5)	$O_{1.00}$
O6	ElbK-13	0.19336(4)	0.18294(4)	−0.20621(8)	0.00750(9)	$O_{1.00}$
	ElbK-9	0.1937(1)	0.1832(1)	−0.2055(2)	0.0086(3)	$O_{1.00}$
	ElbK-11	0.1943(1)	0.1839(1)	−0.2047(2)	0.0090(3)	$O_{1.00}$
O7	ElbK-13	0.28686(4)	0.28627(4)	0.09477(8)	0.00752(9)	$O_{1.00}$
	ElbK-9	0.2858(1)	0.2856(1)	0.0938(2)	0.0084(3)	$O_{1.00}$
	ElbK-11	0.2851(1)	0.2852(1)	0.0936(2)	0.0087(3)	$O_{1.00}$
O8	ElbK-13	0.20939(4)	0.27003(5)	0.45584(8)	0.00710(9)	$O_{1.00}$
	ElbK-9	0.2094(1)	0.2697(1)	0.4565(2)	0.0077(3)	$O_{1.00}$
	ElbK-11	0.2094(1)	0.2697(1)	0.4570(2)	0.0079(3)	$O_{1.00}$

Note: For definition of U_{eq} see Fischer and Tillmanns (1988).

TABLE 4. Selected interatomic distances (Å) in tourmaline crystals of synthetic B-rich olenite

	ElbK-13	ElbK-9	ElbK-11
X-O2 (×3)	2.533(2)	2.532(4)	2.505(4)
X-O4 (×3)	2.779(1)	2.771(1)	2.773(3)
X-O5 (×3)	2.691(1)	2.684(3)	2.687(3)
Mean	2.668	2.662	2.655
Y-O1	1.8971(9)	1.906(2)	1.920(3)
Y-O2 (×2)	1.9520(6)	1.947(2)	1.950(2)
Y-O3	2.0912(11)	2.098(3)	2.101(3)
Y-O6 (×2)	1.9316(7)	1.933(2)	1.939(2)
Mean	1.959	1.961	1.967
Z-O3	1.9661(5)	1.963(1)	1.959(1)
Z-O6	1.8844(7)	1.884(2)	1.879(2)
Z-O7	1.8811(6)	1.885(2)	1.884(2)
Z-O7′	1.9314(6)	1.935(2)	1.935(2)
Z-O8	1.8817(6)	1.880(2)	1.876(2)
Z-O8′	1.8953(7)	1.892(2)	1.890(2)
Mean	1.907	1.907	1.904
T-O4	1.6106(4)	1.602(1)	1.595(1)
T-O5	1.6290(5)	1.628(2)	1.625(1)
T-O6	1.6129(7)	1.600(2)	1.591(2)
T-O7	1.6034(6)	1.591(2)	1.583(2)
Mean	1.614	1.605	1.599
B-O2	1.366(2)	1.360(4)	1.356(4)
B-O8 (×2)	1.3742(9)	1.377(2)	1.374(3)
Mean	1.371	1.371	1.368

RESULTS AND DISCUSSION

Crystal chemistry

The seed crystal (from the Hercules mine), on which sample ElbK-11 was grown, has been also analyzed by the current authors. The composition of the seed crystal is $^{X}(Na_{0.70}Ca_{0.06}K_{0.01}\square_{0.23})$ $^{Y}(Fe^{2+}_{1.43}Al_{1.10}Mg_{0.44}Mn^{2+}_{0.02}Ti^{4+}_{0.01})^{Z}(Al_{5.20}Mg_{0.80})(BO_3)_3[Si_{5.94}Al_{0.06}O_{18}]$ $^{V}(OH)_3{}^{W}[(OH)_{0.86}O_{0.09}F_{0.05}]$ [a = 15.959(1), c = 7.188(1) Å]. Hence, this tourmaline belongs to the schorl-dravite series and has a dominant schorl component. The lattice parameters of the other seed crystals are similar within the limits of error. The

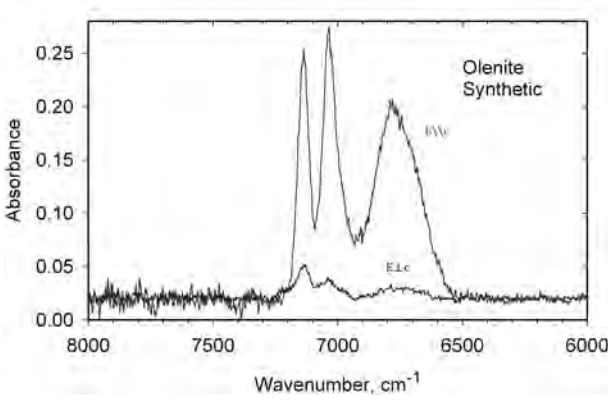

FIGURE 1. Near infrared spectra of synthetic B-rich olenite (sample ElbK-11) in the OH overtone region.

olenite was growing faster at the +*c* pole of the seed tourmaline crystals (up to ~1 mm thick olenite overgrowth). Samples of these colorless olenite overgrowths were separated, structurally examined, and finally chemically analyzed. The optimized formulas of the overgrown tourmaline samples were calculated by using the refined $^{[4]}$B. Recently, Lussier et al. (2011) investigated liddicoatite samples from Anjanaboina, Madagascar, which contain essentially no $^{[4]}$B. They got consistent refinement results compared with their ^{11}B MAS NMR spectroscopy data by using an ionized scattering-curve for O and a neutral scattering-curve for Si. We believe that this is an appropriate method for investigations of tourmalines, which contain no or relatively low amounts of $^{[4]}$B. Previous investigations by Ertl et al. (1997) on natural B-rich olenite show that, within errors, the refined value of $^{[4]}$B, determined with the Z site fixed at full occupancy (Al_6), is in agreement with the amount estimated by ^{11}B MAS NMR spectroscopy data on bulk material of that inhomogeneous tourmaline (Marler and Ertl 2002; Lussier et al. 2009). Because SIMS analysis of B gives the value of both $^{[3]}$B + $^{[4]}$B, the uncertainty in the amount of $^{[4]}$B is larger than that from the X-ray refinement that refines only the T site. Hence, the refined value of $^{[4]}$B was taken as correct, and the T site was set to: T = (Si_{EMP}, B_{SREF}, $Al_{6\text{-}Si\text{-}B}$), where the value of B_{SREF} was slightly corrected for the $^{[4]}$Al content, because Al has only 13 e^-, whereas Si has 14 e^-. Hence, the total electrons of the refinement Si↔B are in agreement with the final T-site occupancy. For the final optimized formulas Al_2O_3 and H_2O were calculated iteratively for Y + Z + T = 15 apfu and to reach a total sum of 100%. The final formulas are

ElbK-13: $^{X}(Na_{0.65}Ca_{0.01}\square_{0.34})^{Y}(Al_{2.47}Li_{0.44}Fe^{2+}_{0.06}Ti^{4+}_{0.03})$
$^{Z}Al_6(BO_3)_3[Si_{5.20}B_{0.54}Al_{0.26}O_{18}]^{V}[(OH)_{2.90}O_{0.10}]^{W}[O_{0.90}(OH)_{0.10}]$;

ElbK-9: $^{X}(Na_{0.69}Ca_{0.01}\square_{0.30})^{Y}(Al_{2.42}Li_{0.53}Ti^{4+}_{0.03}Fe^{2+}_{0.02})$
$^{Z}Al_6(BO_3)_3[Si_{4.82}B_{0.90}Al_{0.28}O_{18}]^{V}(OH)_3{}^{W}[(OH)_{0.50}O_{0.49}F_{0.01}]$;

ElbK-11: $^{X}(Na_{0.63}Ca_{0.04}\square_{0.33})^{Y}(Al_{2.23}Li_{0.49}Fe^{2+}_{0.22}Zn_{0.02}Mg_{0.02}Ti^{4+}_{0.02})$
$^{Z}Al_6(BO_3)_3[Si_{4.65}B_{1.19}Al_{0.16}O_{18}]^{V}(OH)_3{}^{W}[(OH)_{0.85}O_{0.14}F_{0.01}]$.

The analyzed SIMS values of B_2O_3 (Table 1) are within a relative error of only 1–6% in excellent agreement with the optimized values, which were derived from the refinement (Table 4). The calculated value of Al_2O_3 is within an error of ≤1.7% consistent with the measured value. The relatively high sums of Y + Z + T for the measured data can be explained due to the slightly too high values of B_2O_3 and too low values of H_2O (Table 1). Because the crystals used for structure analysis were relatively small, only two spots on them could be used for H_2O analysis. Also matrix effects of the B- and Al-rich tourmalines may have an influence to the H_2O SIMS values. Consequently, the quality of the H_2O SIMS data is less than that of the other components. Near infrared spectra of the B-richest sample (ElbK-11) in the OH overtone region are qualitatively similar to the spectra of another Al-rich tourmaline (rossmanite from Rožná, Czech Republic; Ertl et al. 2005), in which the OH sites are completely occupied by OH (Selway et al. 1998). This would be in agreement with the final formula of ElbK-11, in which the OH sites are almost completely filled up by OH.

By using the SiO_2 values derived from EPMA, we calculated significant values of Al at the T site. This is not surprising because natural olenite from the type locality in Russia and from the Koralpe in Austria also shows significant amounts of $^{[4]}$Al (up to ~0.27 apfu; Hughes et al. 2000; Schreyer et al. 2002; Ertl et al. 2007). Clear evidence for both, $^{[4]}$B and $^{[4]}$Al in tourmaline, was found only in Al-rich tourmalines (olenite, elbaite, fluor-elbaite, liddicoatite, "oxy-rossmanite"), from several localities (Ertl et al. 2005; Lussier et al. 2009). In our investigated synthetic olenites, the amount of $^{[4]}$Al is in the range of 0.16–0.28 apfu (Table 1). The highest amount of Fe (~1.7 wt% FeO; Table 2) was found in sample ElbK-11, which was synthesized at the lowest temperature of these experiments (400 °C). We believe that the Fe-rich seed crystal was partly dissolved at this relatively low temperature, especially at the beginning of the olenite growth, and the released Fe was finally found in the overgrowth.

Crystal structure

Using currently valid tourmaline end-member species (Henry et al. 2011), we can describe this tourmaline sample essentially as a mixture of olenite (37–45 mol%) and rossmanite (30–34 mol%). Hence, these synthetic tourmaline samples belong to the olenite-rossmanite series. Small components of schorl (≤7 mol%) can be explained by a partly dissolved Fe-rich seed tourmaline crystal. The <Y-O> distances with 1.959–1.967 Å (Table 4) of the synthetic olenite samples are similar to natural olenite (1.957–1.969 Å; Ertl et al. 1997; Schreyer et al. 2002).

The <T-O> distance with 1.599–1.614 Å (Table 4) is significantly smaller relative to a site fully occupied with Si (~1.620 Å; Hawthorne 1996; MacDonald and Hawthorne 1995; Bloodaxe et al. 1999; Ertl et al. 2001). A substitution of Al^{3+} for Si^{4+} was first proposed by Buerger et al. (1962). The relationship between <T-O> distances and Al occupancy in the ring was first described by Foit and Rosenberg (1979) and Foit (1989). MacDonald and Hawthorne (1995) were able to improve this relationship due to high-quality structure refinement (SREF) data. A significant substitution of B^{3+} for Si^{4+} in a natural tourmaline was described by Ertl et al. (1997) for the first time. The optimized formulas for the synthetic olenites show the T site to be occupied by ($Si_{5.20}B_{0.54}Al_{0.26}$) (ElbK-13), ($Si_{4.82}B_{0.90}Al_{0.28}$) (ElbK-9), and ($Si_{4.65}B_{1.19}Al_{0.16}$) (ElbK-11), respectively, which is in a good

agreement with the observed <T-O> distance. Ertl et al. (2001) provided a formula to calculate the <T-O> distance by using the T-site occupants. By using the updated formula (Ertl et al. 2007) the calculated <T-O> distances are similar to the observed <T-O> distances (Table 4) within an error of ≤0.1%. However, we are able to improve this formula to

$$< \text{T-O} >= \left(\frac{x_A \times r_A + x_B \times r_B + x_C \times r_C + \ldots}{6} - 0.26\,\text{Å} \right) \times 0.79 + 1.620\,\text{Å}$$

where: r_A, ... = effective ionic radius of atom [4]A, …, in angstroms (Si: 0.26, Al: 0.39, B: 0.11; Shannon 1976); x_A, ... = Concentration (apfu) of element A, which occupies the T site of tourmaline. Note that the sum of all elements at the T site is 6.00 apfu; <T-O> = average T-O bond length (Å) of tourmaline.

We observed a very good agreement between the calculated <T-O> distances and values derived from Rietfeld refinement by the application of this formula to the T-site occupations of the synthetic olenites (with up to ~2 apfu [4]B) published by Marler et al. (2002) and Kempl et al. (2009).

An H atom (H3) at the site associated with O3 was easily located in this refinement. Ertl et al. (2002) showed that the bond-angle distortion (σ^2_{oct}) of the ZO_6 octahedron in a tourmaline is largely a function of the <Y-O> distance of that tourmaline, although the occupant of the O3 site (V position in the general formula) also affects that distortion. The covariance, *r*, of <Y-O> and σ^2_{oct} of the ZO_6 octahedron is –0.99 (Fig. 2 in Ertl et al. 2005) for all investigated tourmalines that are occupied by three (OH) groups. In Figure 2, only olenite sample ElbK-13 shows a slight tendency toward the composition of buergerite from San Luis Potosi, Mexico [which contains 0.3 (OH) and 2.7 O at the V site; Dyar et al. 1998], the other synthetic samples lie approximately on the V site = 3 (OH) line. Hence, the V site of samples ElbK-9 and ElbK-11 is completely occupied by (OH), only sample ElbK-13 shows a slight deficiency in (OH). This is in agreement with the final formula of this sample, which contains a relatively low amount of (OH) (Table 1).

A pronounced negative correlation (r^2 = 1.00 for only 3 data points; Fig. 3) between temperature during crystal growth and [4]B (from refinement) in synthetic olenite was found (all investigated samples were synthesized at 260 MPa H_2O). Such a correlation is in good agreement with Schreyer et al. (2000), Marler et al. (2002), Ertl et al. (2008), and Kempl et al. (2009) who had shown that toward lower temperatures higher contents of [4]B are found in synthetic tourmaline. The observations of Ertl et al. (2008) and Kempl et al. (2009) indicated that the [4]B content does not change significantly with pressure at a given temperature.

An excellent negative correlation between tetrahedrally coordinated B in Al- and B-rich tourmaline and the unit-cell volume was described by Marler et al. (2002). We were able to improve this correlation for Li-bearing tourmalines by using only data derived from high-quality single-crystal structure analyses. In Figure 4, we present the relationship between tetrahedrally coordinated B (from refinement) in Al- and B-rich, Li-bearing, and Ca-poor tourmaline and the unit-cell volume (r^2 = 0.990). This correlation will be helpful to get a good estimation of [4]B (relative error to the refined values is smaller than ±10%) in natural Al-rich and Li-bearing tourmalines (with a low Ca content) where only the lattice parameters are known. The formula for calculating the tetrahedral B is: [4]B = (1533.5 – V)/16.801 (cell volume V in Å^3; [4]B in apfu).

Another interesting correlation is the relationship between <X-O> and <Z-O> distance in natural and synthetic olenite. For this correlation only data from single-crystal structures of natural and synthetic olenite samples (with Mg ≤ 0.1 apfu) was included (this work; Ertl et al. 2003, 2004, 2007; Hughes et al. 2000; Schreyer et al. 2002). Although the Z site is only occupied by Al, the <Z-O> distance varies significantly. The <X-O> and <Z-O> distance are positively correlated [r^2 = 0.8(1)], which can maybe explained by inductive effects in the crystal structure. However, more high-quality structural data and more investigations are necessary for a better understanding of this correlation.

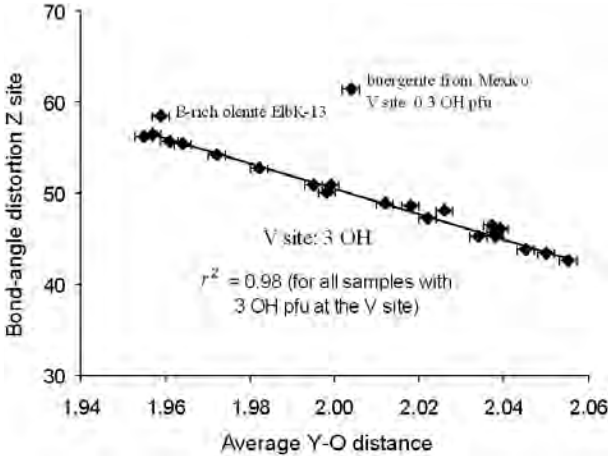

FIGURE 2. Relationship between bond-angle distortion (σ^2_{oct}; definition in Ertl et al. 2002) of the ZO_6 octahedron and the average Y-O distance. Modified from Figure 3 of Ertl et al. (2002), including the structural data from Hughes et al. (2004).

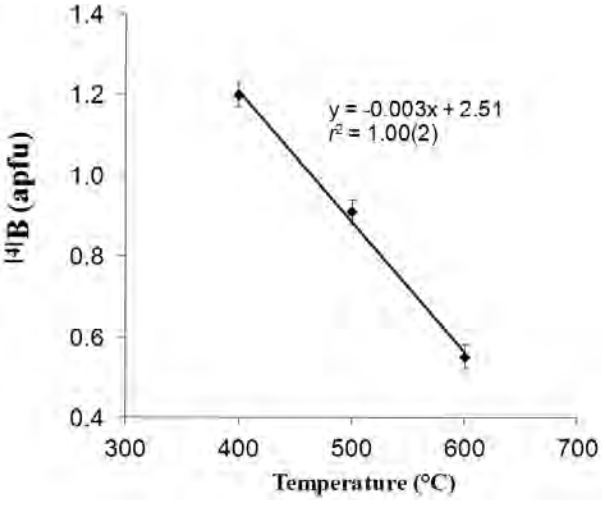

FIGURE 3. Relationship between temperature during crystal growth and [4]B (from refinement) in synthetic olenite. All samples were synthesized at 260 MPa H_2O. The error of the temperature is smaller than the symbols (±2 °C).

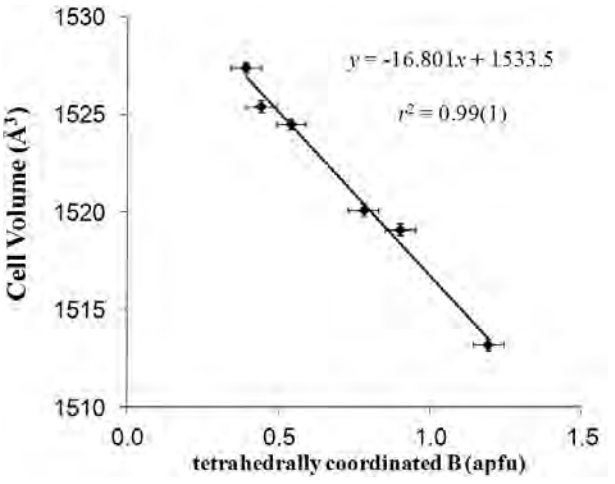

FIGURE 4. Relationship between tetrahedrally coordinated boron (from refinement) in Al- and [4]B-rich, Li-bearing tourmaline and the unit-cell volume. Note: Natural and synthetic Al- and [4]B-rich Li-bearing tourmaline samples (refined [4]B ≥0.4 apfu; Ca ≤0.10 apfu; Li: 0.4–1.0 apfu; FeO + MnO <2.0 wt%; with a cell volume <1530 Å^3) were plotted (this study; Ertl et al. 2007, 2008; Lussier et al. 2008). Only samples were used that were also characterized by single-crystal structural studies.

ACKNOWLEDGMENTS

We greatly thank David London, University of Oklahoma, for providing the excellent synthetic tourmaline samples. Without the work of David London and George B. Morgan VI, University of Oklahoma, this study would not have been possible. This work was funded by the Austrian Science Fund (FWF) project no. P23012-N19 to A.E. and National Science Foundation grant EAR-0947956 to G.R.R. We thank Aaron J. Lussier and an anonymous reviewer for their careful reviews of the manuscript.

REFERENCES CITED

Buerger, M.J., Burnham, C.W., and Peacor, D.R. (1962) Assessment of the several structures proposed for tourmaline. Acta Crystallographica, 15, 583–590.

Bloodaxe, E.S., Hughes, J.M., Dyar, M.D., Grew, E.S., and Guidotti, C.V. (1999) Linking structure and chemistry in the schorl-dravite series. American Mineralogist, 84, 922–928.

Dyar, M.D., Taylor, M.E., Lutz, T.M., Francis, C.A., Guidotti, C.V., and Wise, M. (1998) Inclusive chemical characterization of tourmaline: Mössbauer study of Fe valence and site occupancy. American Mineralogist, 83, 848–864.

Dyar, M.D., Wiedenbeck, M., Robertson, D., Cross, L.R., Delaney, J.S., Ferguson, K., Francis, C.A., Grew, E.S., Guidotti, C.V., Hervig, R.L., and others. (2001) Reference minerals for the microanalysis of light elements. Geostandards Newsletter, 25, 441–463.

Ertl, A., Pertlik, F., and Bernhardt, H.-J. (1997) Investigations on olenite with excess boron from the Koralpe, Styria, Austria. Österreichische Akademie der Wissenschaften, Mathematisch-naturwissenschaftliche Klasse, Abteilung I, Anzeiger, 134, 3-10, Wien.

Ertl, A., Hughes, J.M., and Marler, B. (2001) Empirical formulae for the calculation of <*T*-O> and *X*-O2 bond lengths in tourmaline and relations to tetrahedrally-coordinated boron. Neues Jahrbuch Mineralogie Monatshefte, 12, 548–557.

Ertl, A., Hughes, J.M., Pertlik, F., Foit, F.F. Jr., Wright, S.E., Brandstätter, F., and Marler, B. (2002) Polyhedron distortions in tourmaline. Canadian Mineralogist, 40, 153–162.

Ertl, A., Hughes, J.M., Prowatke, S., Rossman, G.R., London, D., and Fritz, E.A. (2003) Mn-rich tourmaline from Austria: structure, chemistry, optical spectra, and relations to synthetic solid solutions. American Mineralogist, 88, 1369–1376.

Ertl, A., Pertlik, F., Dyar, M.D., Prowatke, S., Hughes, J.M., Ludwig, T., and Bernhardt, H.-J. (2004) Fe-rich olenite with tetrahedrally coordinated Fe^{3+} from Eibenstein, Austria: Structural, chemical, and Mössbauer data. Canadian Mineralogist, 42, 1057–1063.

Ertl, A., Rossman, G.R., Hughes, J.M., Prowatke, S., and Ludwig, T. (2005) Mn-bearing "oxy-rossmanite" with tetrahedrally coordinated Al and B from Austria: Structure, chemistry, and infrared and optical spectroscopic study. American Mineralogist, 90, 481–487.

Ertl, A., Hughes, J.M., Prowatke, S., Ludwig, T., Prasad, P.S.R., Brandstätter, F., Körner, W., Schuster, R., Pertlik, F., and Marschall, H. (2006) Tetrahedrally-coordinated boron in tourmalines from the liddicoatite-elbaite series from Madagascar: Structure, chemistry, and infrared spectroscopic studies. American Mineralogist, 91, 1847–1856.

Ertl, A., Hughes, J.M., Prowatke, S., Ludwig, T., Brandstätter, F., Körner, W., and Dyar, M.D. (2007) Tetrahedrally-coordinated boron in Li-bearing olenite from "mushroom" tourmaline from Momeik, Myanmar: Structure and chemistry. Canadian Mineralogist, 45, 891–899.

Ertl, A., Tillmanns, E., Ntaflos, T., Francis, C., Giester, G., Körner, W., Hughes, J.M., Lengauer, C., and Prem, M. (2008) Tetrahedrally coordinated boron in Al-rich tourmaline and its relationship to the pressure–temperature conditions of formation. European Journal of Mineralogy, 20, 881–888.

Ertl, A., Kolitsch, U., Meyer, H.-P., Ludwig, T., Lengauer, C.L., Nasdala, L., and Tillmanns, E. (2009) Substitution mechanism in tourmalines of the "fluor-elbaite"-rossmanite series from Wolkenburg, Saxony, Germany. Neues Jahrbuch Mineralogie Abhandlungen, 186, 51–61.

Fischer, R.X. and Tillmanns, E. (1988) The equivalent isotropic displacement factor. Acta Crystallographica, C44, 775–776.

Foit, F.F. Jr. (1989) Crystal chemistry of alkali-deficient schorl and tourmaline structural relationships. American Mineralogist, 74, 422–431.

Foit, F.F. Jr. and Rosenberg, P.E. (1979) The structure of vanadium-bearing tourmaline and its implications regarding tourmaline solid solutions. American Mineralogist, 64, 788–798.

Hawthorne, F.C. (1996) Structural mechanisms for light-element variations in tourmaline. Canadian Mineralogist, 34, 123–132.

Hawthorne, F.C. and Henry, D.J. (1999) Classification of the minerals of the tourmaline group. European Journal of Mineralogy, 11, 201–215.

Hawthorne, F.C., MacDonald, D.J., and Burns, P.C. (1993) Reassignment of cation site-occupancies in tourmaline: Al-Mg disorder in the crystal structure of dravite. American Mineralogist, 78, 265–270.

Henry, D., Novák, M., Hawthorne, F.C., Ertl, A., Dutrow, B.L., Uher, P., and Pezzotta, F. (2011) Nomenclature of the tourmaline-supergroup minerals. American Mineralogist, 96, 895–913.

Hughes, J.M., Ertl, A., Dyar, M.D., Grew, E.S., Shearer, C.K., Yates, M.G., and Guidotti, C.V. (2000) Tetrahedrally coordinated boron in a tourmaline: boron-rich olenite from Stoffhütte, Koralpe, Austria. Canadian Mineralogist, 38, 861–868.

Hughes, J.M., Ertl, A., Dyar, M.D., Grew, E., Wiedenbeck, M., and Brandstätter, F. (2004) Structural and chemical response to varying [4]B content in zoned Fe-bearing olenite from Koralpe, Austria. American Mineralogist, 89, 447–454.

Kempl, J. (2008) Synthese und Charakterisierung von Turmalin mit tetraedrischem Bor. Diploma Thesis, Technische Universität Berlin, 85 p.

Kempl, J., Wunder, B., Koch-Müller, M., and Rhede, D. (2009) Quantification of the [4]B-content in synthetic tourmaline: A multi-methodical study. DMG Meeting 2009, Halle, Germany, 13.09.-16.09.2009, Abstract 104 (CD-ROM).

London, D. (2011) Experimental synthesis and stability of tourmaline: a historical overview. Canadian Mineralogist, 49, 117–136.

London, D. and Morgan, G.B. VI (2011) Synthesis and stability of elbaite. (abstr.) GAC-MAC-SEG-SGA Joint Annual Meeting, Ottawa, May 25-27, Abstracts, 34, 123.

Ludwig, T. and Stalder, R. (2007) A new method to eliminate the influence of in-situ contamination in SIMS analysis of hydrogen. Journal of Analytical Atomic Spectrometry, 22, 1415–1419.

Lussier, A.J., Aguiar, P.M., Michaelis, V.K., Kroeker, S., Herwig, S., Abdu, Y., and Hawthorne, F.C. (2008) Mushroom elbaite from the Kat Chay mine, Momeik, near Mogok, Myanmar: I. Crystal chemistry by SREF, EMPA, MAS NMR and Mössbauer spectroscopy. Mineralogical Magazine, 72, 747–761.

Lussier, A.J., Aguiar, P.M., Michaelis, V.K., Kroeker, S., and Hawthorne, F.C. (2009) The occurrence of tetrahedrally coordinated Al and B in tourmaline: An ^{11}B and ^{27}Al MAS NMR study. American Mineralogist, 94, 785–792.

Lussier, A.J., Abdu, Y., Hawthorne, F.C., Michaelis, V.K., and Kroeker, S. (2011) Oscillatory zoned liddicoatite from Anjanabonoina, Central Madagascar I. Crystal chemistry and structure by SREF and ^{11}B and ^{27}Al MAS NMR spectroscopy. Canadian Mineralogist, 49, 63–88.

MacDonald, D.J. and Hawthorne, F.C. (1995) The crystal chemistry of Si ⇔ Al substitution in tourmaline. Canadian Mineralogist, 33, 849–858.

Marler, B. and Ertl, A. (2002) Nuclear magnetic resonance and infrared spectroscopic study of excess-boron olenite from Koralpe, Styria, Austria. American Mineralogist, 87, 364–367.

Marler, B., Borowski, M., Wodara, U., and Schreyer, W. (2002) Synthetic tourmaline (olenite) with excess boron replacing silicon in the tetrahedral site: II. Structure analysis. European Journal of Mineralogy, 14, 763–771.

Ottolini, L. and Hawthorne, F.C. (1999) An investigation of SIMS matrix effects on H, Li and B ionization in tourmaline. European Journal of Mineralogy, 11, 679–690.

Ottolini, L., Bottazzi, P., and Vannucci, R. (1993) Quantification of lithium, beryllium, and boron in silicates by secondary ion mass spectrometry using

conventional energy filtering. Analytical Chemistry, 65, 1960–1968.
Otwinowski, Z., Borek, D., Majewski, W., and Minor, W. (2003) Multiparametric scaling of diffraction intensities. Acta Crystallographica, A59, 228–234.
Pearce, N., Perkins, W.T., Westgate, J.A., Gorton, M.P., Jackson, S.E., Neal, C.R., and Chenery, S.P. (1997) A compilation of new and published major and trace element data for NIST SRM 610 and NIST SRM 612 glass reference materials. Geostandards Newsletter, 21, 115–144.
Pouchou, J.L. and Pichoir, F. (1985) "PAP" $\phi(\rho z)$ correction procedure for improved quantitative microanalysis. In J.T. Armstrong, Ed., Microbeam Analysis, p. 104–106. San Francisco Press, California.
Schlager, O. (2003) Hochdruck-Niedertemperatursynthesen von extreme borreichen olenitischen Turmalinen. Diploma Thesis, Ruhr-Universität Bochum, 78 p.
Schreyer, W., Wodara, U., Marler, B., van Aken, P.A., Seifert, F., and Robert, J.L. (2000) Synthetic tourmaline (olenite) with excess boron replacing silicon in the tetrahedral site: I. synthesis conditions, chemical and spectroscopic evidence. European Journal of Mineralogy, 12, 529–541.
Schreyer, W., Ertl, A., Hughes, J., Bernhardt, H.-J., Kalt, A., and Prowatke, S. (2002) Tetrahedral boron in olenite from the type locality: A chemical and structural investigation. European Journal of Mineralogy, 14, 935–942.
Selway, J. B., Novák, M., Hawthorne, F., Černý, P., Ottolini, L., and Kyser, T.K. (1998) Rossmanite, $\square(LiAl_2)Al_6(Si_6O_{18})(BO_3)_3(OH)_4$, a new alkali-deficient tourmaline: Description and crystal structure. American Mineralogist, 83, 896–900.
Shannon, R.D. (1976) Revised effective ionic radii and systematic studies of interatomic distances in halides and chalcogenides. Acta Crystallographica, A32, 751–767.
Sheldrick, G.M. (1997) SHELXL-97, a program for crystal structure refinement. University of Göttingen, Germany.

Manuscript received November 23, 2011
Manuscript accepted May 31, 2012
Manuscript handled by Andrew McDonald